*29th EPS Conference on Plasma Phys. and Contr. Fusion Montreux, 17-21 June 2002 ECA Vol. **26B**, P-1.082 (2002)*

Gyrokinetic Calculations of Microinstabilities and Transport during RF H-modes on Alcator C-MOD

M. H. Redi[a], C. Fiore[b], P. Bonoli[b], C. Bourdelle[a], R. Budny[a], W. D. Dorland[c], D. Ernst[b], G. Hammett[a], D. Mikkelsen[a], J. Rice[b], S. Wukitch[b]

[a]*Princeton Plasma Physics Laboratory, Princeton, NJ 08540, USA*
[b]*Plasma Science and Fusion Center, MIT, Cambridge, MA 02139, USA*
[c]*Institute for Plasma Research, U. MD, College Park, MD 20742, USA*

Introduction

Physics understanding for the experimental improvement of particle and energy confinement is being advanced through massively parallel calculations of microturbulence for simulated plasma conditions. The ultimate goal, an experimentally validated, global, nonlocal, fully nonlinear calculation of plasma microturbulence is still not within reach, but extraordinary progress has been achieved in understanding microturbulence, driving forces and the plasma response in recent years.

In this paper we discuss gyrokinetic simulations of plasma turbulence[1,2] being carried out to examine a reproducible, H-mode, RF heated experiment on the Alcator C-MOD tokamak[3], which exhibits an internal transport barrier (ITB)[4,5,6,7]. This off axis RF case represents the early phase of a very interesting dual frequency RF experiment, which shows density control with central RF heating later in the discharge. The ITB exhibits steep, spontaneous density peaking: a reduction in particle transport occurring without a central particle source. Since the central temperature is maintained while the central density is increasing, this also suggests a thermal transport barrier exists. TRANSP analysis shows that χ_{eff} drops inside the ITB[6]. Sawtooth heat pulse analysis also shows a localized thermal transport barrier[7]. For this ICRF EDA H-mode, the minority resonance is at $r/a \geq 0.5$ on the high field side. There is a normal shear profile, with q monotonic.

TRANSP analysis is used to set initial conditions, with T_i not assumed equal to measured T_e, but rather T_i is found from HIREX spectroscopic and neutron data on Alcator C-MOD.and is consistent with $\chi_i \sim \chi^{Chang\text{-}Hinton}$. The simulations, which solve the gyrokinetic Vlasov-Maxwell system, are run out for 10,000 time steps, until the microinstability growth rates, γ, and real frequencies, ω, are verified to have converged and the usual measure of the electrostatic potential, $ln|\phi|^2$, is verified to be linearly increasing, in cases that are designated unstable. **E×B** shearing rates have been estimated from measurements of toroidal rotation but are not of concern here because at the time of interest, the toroidal rotation is near zero, changing from strong co to counter rotation as the ITB is established.

Simulations with the GS2 Gyrokinetic Microstability Code

Linear, fully electromagnetic, gyrokinetic, flux tube calculations of microturbulence for four species (hydrogen, deuterium, boron and electrons) are being used to examine the early stage of formation of the ITB, before a steep electron density gradient is established (Fig. 1). At this point in time, microturbulent instability for three plasma radii is simulated, yielding predicted behavior inside, at and outside the ITB, at radii located at r/a=0.25, 0.45, 0.65 for zones 5, 9 and 13 of 20 equally spaced radial zones. The sensitivity of the microturbulent stability has been examined through the sensitivity of the calculated real frequencies and growth rates to particular driving forces across the plasma (Fig. 2)

The simulations were carried out on the NERSC T3E supercomputer, using 40-64 parallel processors. We obtain microturbulent growth rates for values of $k_\perp\rho_i$ from 0.1 to 80 including the influences of ITG, TEM and ETG modes (Figs. 3 and 4). The stability analysis shows that just inside the barrier (r/a~0.45) no mode is strongly growing for $0.2<k_\perp\rho_i<0.8$. Outside the ITB a clear signature is found for the toroidal ion temperature gradient mode. In the plasma core, modes with $\omega<0$ are unstable at $k_\perp\rho_i \leq 0.4$; there are no strongly growing modes at $0.5\leq k_\perp\rho_i \leq 0.8$. The apparently unstable mode at $k_\perp\rho_i=0.1$ is not converged and does not have a well defined eigenfunction. At higher values of $k_\perp\rho_i$, the TEM (usually found near $k_\perp\rho_i\sim 1$) is not unstable, while the ETG (peaked at $k_\perp\rho_i\sim 25$) is strongly unstable at, and outside the barrier, and stable in the core (Fig. 3,4). Anomalous χ_i is associated with ITG so that we expect reduced ion thermal confinement at, and within the ITB. Anomalous χ_e is associated with strong ETG, and the mixing length model would predict 1/2 for the ratio of χ_e at the ITB to that outside. Sawtooth heat pulse propagation measurements of similar experiments have shown that the effective $\chi^{heatpulse}$ is reduced (by factor~10) in a narrow radial region of ~1 cm, located near the foot of the particle barrier, but not necessarily within the barrier[7]. Reduced microinstability growth rates predicted at the barrier are consistent with the observed reduced transport.

Sensitivity Studies

Figure 2 shows the radial variaton of drift mode driving and stabilizing parameters for the experiment at the time of interest. It is found that either decreasing the plasma electron density gradient or increasing the plasma electron temperature gradient causes the ITG mode to be destabilized in the transport barrier region. The growth rates are more strongly elevated (factor 25) by doubling $(\nabla T_e)/T_e$ than by reducing $(\nabla n_i)/n_i$ by 2. We also find that η_i increases as *r/a* increases, as does the normalized electron temperature gradient. These and the increasing inverse gradient for the primary impurity, boron (4%), may be stabilizing the ITG in the core. The role of magnetic shear, increasing with *r/a*, is still to be examined.

Conclusions

Just before ITB formation, conditions have been established for which a peaked density profile can occur and will persist. Ware pinch provides sufficient fueling to account for a sustained ITB peaked density profile[7]. Microturbulent driving forces are not strong enough to provide anomalous transport through the barrier, since there are no strong instabilities at the ITB. Outside the barrier, ITG and ETG modes are linearly unstable. The sensitivity studies suggest that the observation of ITB with off-axis but not on-axis RF, is due to weaker $(\nabla T_e)/T_e$ at the barrier. However, ITB also occurs spontaneously in the C-MOD ohmic H-mode[4]. The full story will require a detailed examination and comparison of the many driving and damping forces operating in both of these intriguing experiments.

Acknowledgement

We are glad to acknowledge the experimental and diagnostic teams at Alcator C-MOD which provided the data and basis for the analysis in this paper. Research supported by U. S. DOE Contract DE-AC02-76CH03073.

1. M. Kotschenreuther, *et al*., Comp. Phys. Comm. **88**, 128 (1995).
2. W. Dorland, *et. al*., Phys. Rev. Lett. **85**, 5579 (2000).
3. I. H. Hutchinson *et al*., Phys. Plas. **1**, 1511 (1994).
4. C. L. Fiore, *et al*. Phys. Plas. **8,** 2023 (2001).
5. J. Rice*, et al.*, Nuclear Fusion, in press (2002).
6. P. Bonoli, *et. al,* 18th IAEA, Sorrento, Italy, IAEA-CN-77, EXP4/01 (Oct.,2000.)
7. S. Wukitch, *et al.,* Phys. Plas. **9**, 2149 (2002).

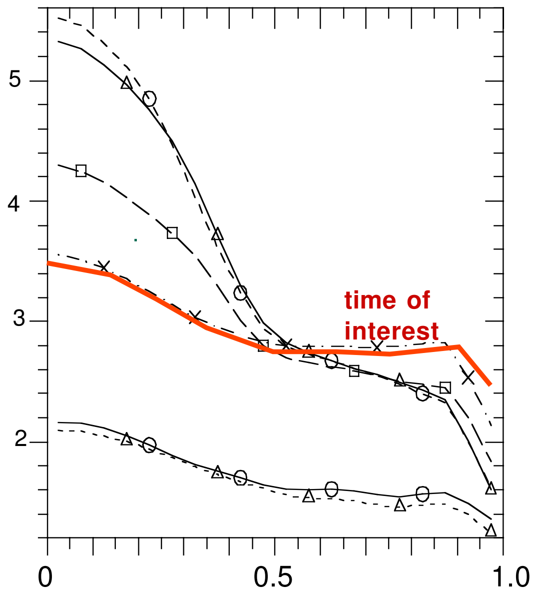

Fig. 1 Electron density ($10^{14}/cm^3$) versus radius (r/a), showing evolution from ohmic phase to RF Hmode ITB density peaked phase. Timeslices every 0.2sec, from 0.5 to 1.4 sec.

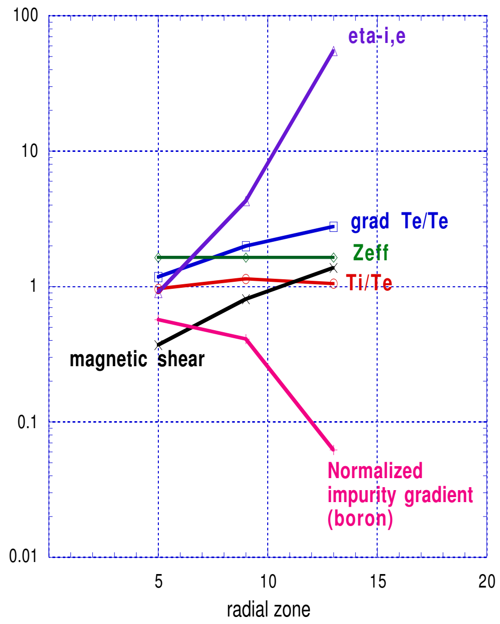

Fig. 2 Normalized driving forces for drift mode microturbulence are balanced to stabilize instabilities inside and at the ITB, compared to outside the ITB

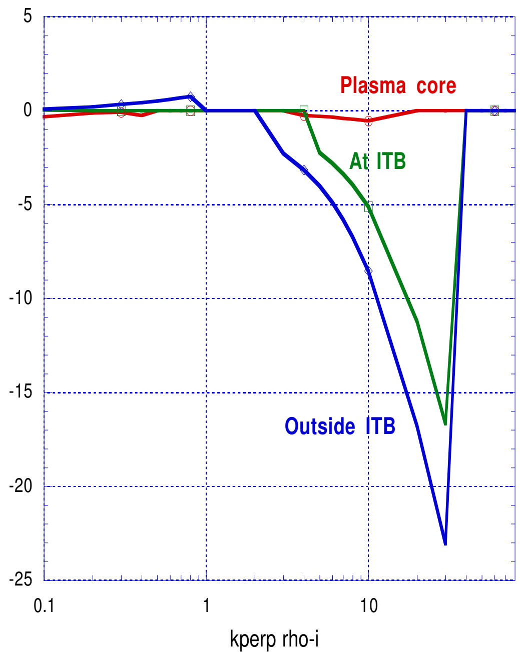

Fig. 3 Real frequencies (~10^6/sec) of drift mode microturbulence inside, at and outside the ITB

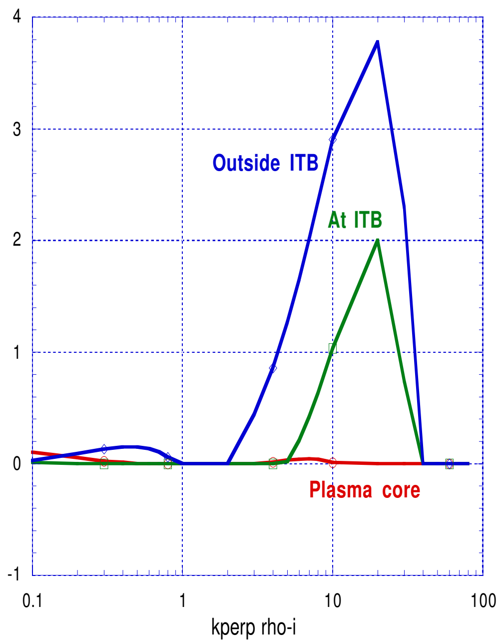

Fig. 4 Real growth rates (~10^6/sec) inside, at and outside the ITB